The International Journal of Advanced Manufacturing Technology (2018) 97:3205–3221
https://doi.org/10.1007/s00170-018-2046-2

ORIGINAL ARTICLE

Research on the flexible support platform for fused deposition modeling

Shen Hongyao [1,2] · Ye Xiaoxiang [1,2] · Fu Jianzhong [1,2]

Received: 19 September 2017 / Accepted: 16 April 2018 / Published online: 23 May 2018

Abstract
Traditional fused deposition modeling (FDM) additive manufacturing technologies usually fabricate a 3D physical model layer by layer. However, support structure under cantilever geometry and model unloading are two major drawbacks of the FDM technology that waste material and hamper the automation of FDM. This paper designs a kind of flexible support platform for assisting FDM to avoid waste and promote automation of FDM, which consists of basic units controlled to rise and fall by the computer. During the printing process, the platform can form different support structures using basic units for different models. When the printing process is finished, basic units rise to unload the model from the platform. Typical models were printed to verify efficiency of support structure reduction, and effects of the model's position on reduction were studied. The automatic unloading of the flexible platform was simulated to study the stress state and then the mechanical test was put into effect to measure the actual value of pressure. In the last part, parameters of unloading successfully are given to guide the unloading process.

Keywords 3D printing · Fused deposition modeling · Flexible platform · Support structure reduction · Automatic unloading

1 Introduction

According to the designed three-dimensional CAD model, 3D printing, a kind of rapid prototyping technology, manufactures parts through accumulation of material layer by layer, called as the core technology of "A third industrial revolution" by the Economist [1]. With great advantages in prototyping and mold manufacturing, 3D printing has been widely applied in fields such as government, aerospace and defense, medical equipment, education and manufacturing industry [2–5]. FDM is mostly used because of being simple to operate and environmental friendly. Scott Crump suggested the principle of FDM in 1988 and Stratasys launched the first commercial model, 3D-Modeler in 1992 [3]. Many improvements have been implemented from then on. Jusung Lee et al. [6] proposed a new inner support structure generation algorithm to reduce the manufacturing time and the amount of material used to fill the interior of an object. Md. Hazrat Ali et al. [7] proposed an extrusion model with five nozzles to improve efficiency of 3D printing. As shown in Fig. 1, a typical FDM printer includes a build platform, a liquefier head with many heating elements, and extrusion nozzles to extrude the material.

As shown in Fig. 2, FDM operation consists of 5 steps [9]. The first step is to design a 3D model using 3D modeling software or reverse engineering techniques. The second step is conversion of data format. STL file format is preferred, which approximates the surface of a 3D model by using triangulation grids. The third step is slicing the model into layers and generating instructions after planning tool paths on each layer in a computer-aided manufacturing (CAM) environment. In the fourth step, a fabrication is undertaken by a 3D printing software automatically. The filament material is partially melted, extruded and deposited by a heated nozzle. The material cools, solidifies, and sticks with surrounding materials. A wide range of materials are available for this manufacturing process such as acrylonitrile butadiene styrene (ABS), polycarbonate (PC), and PC-ABS blend. The last step is removing the solid model from the platform and doing the post-processing.

Though FDM shows an immense potential in manufacturing compared to conventional polymer processing techniques,

✉ Shen Hongyao
shenhongyao@zju.edu.cn

[1] State Key Laboratory of Fluid Power and Mechatronic Systems, College of Mechanical Engineering, Zhejiang University, Hangzhou 310027, China

[2] Key Laboratory of 3D Printing Process and Equipment of Zhejiang Province, College of Mechanical Engineering, Zhejiang University, Hangzhou 310027, China

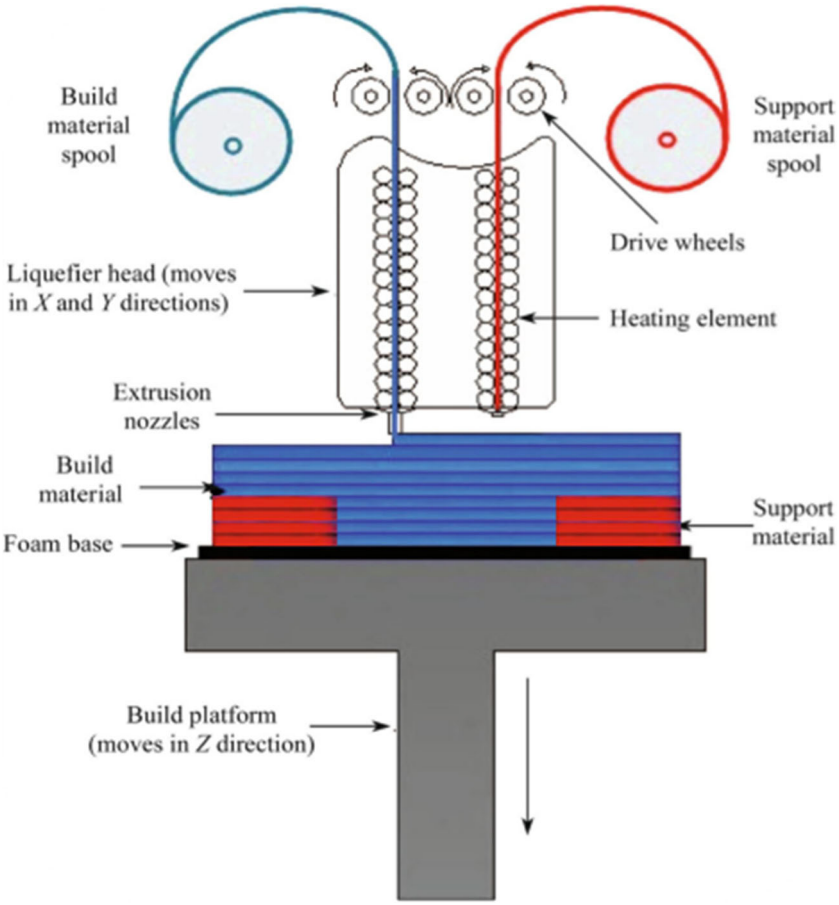

Fig. 1 An illustration of FDM printer [8]

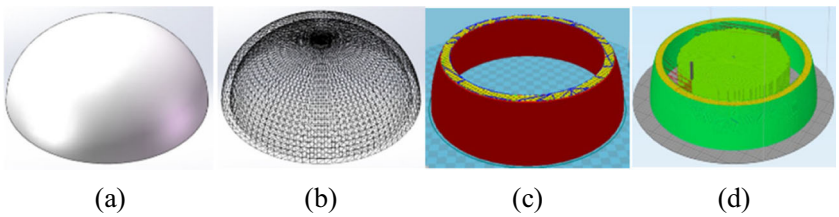

Fig. 2 Steps of FDM operation. **a** Designing a 3D model. **b** Data format conversion. **c** Slicing and generating instructions. **d** Printing the model

there are two problems standing in the way of development of FDM. One is the support structure, which is generated to support the cantilever structure of the solid model [10]. As shown in Fig. 3, the support structure not only wastes material and consumes printing time, but also increases the roughness of the surface which is in touch with support structure.

The other is model unloading when a solid model finishes printing, which relies on manpower with high requirements on operator's experience in an inefficient way. As shown in Fig. 4, the operator finds the starting point of the printing model, and then uses an art knife and a small shovel to scoop it up from the platform. However, for lack of theoretical

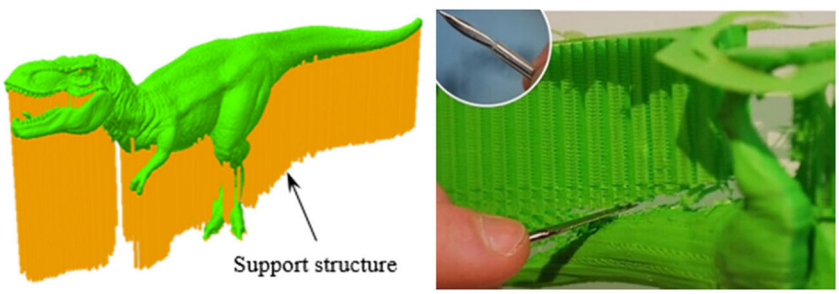

Fig. 3 Support structure under model's cantilever geometry

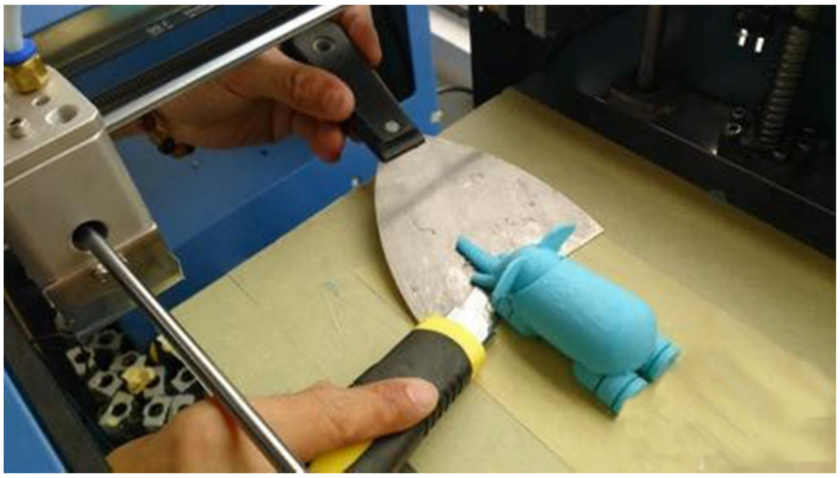

Fig. 4 An illustration of manual model unloading

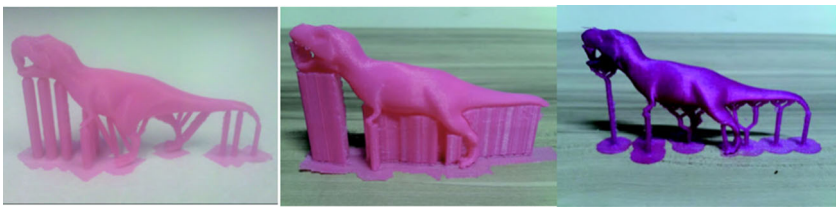

(a) (b) (c)

Fig. 5 Comparisons of printed dinosaur models (height 50 mm) with support structure generated by different algorithms. **a** New algorithm, **b** Cura, **c** Meshmixer [14]

researches, it is still unable to achieve automatic separation and difficult to separate large printing models in this way. It may damage model's fragile structure if operator separates the model rudely. Therefore, it is of great importance to deal with these problems to improve FDM technology.

Present researches on support structure of FDM concentrate on the support algorithm and support materials, and meanwhile some researchers invent new FDM printers to solve this problem. The support algorithm can be concluded to two parts: looking for the parts that need to be supported

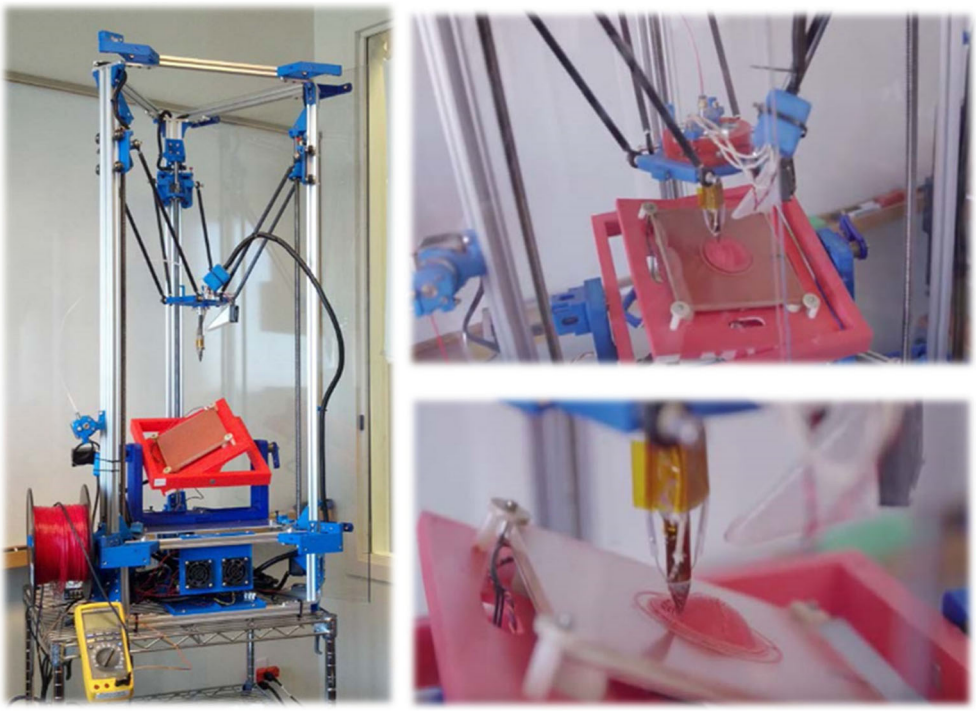

Fig. 6 MERL's 5-axis FDM printer and its printing illustration, showing coordinated motion of all five axes including local control of the nozzle perpendicular [19]

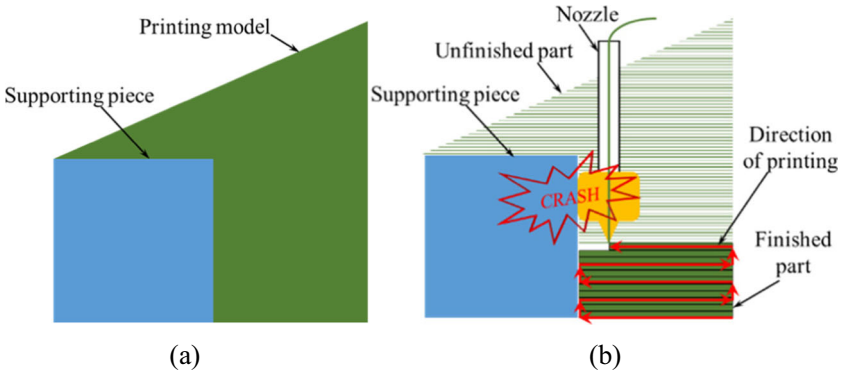

Fig. 7 An illustration of printer's nozzle in a collision with supporting piece during the printing process in the case of putting supporting piece before printing. **a** A printing model with supporting piece. **b** A sketch of the crash

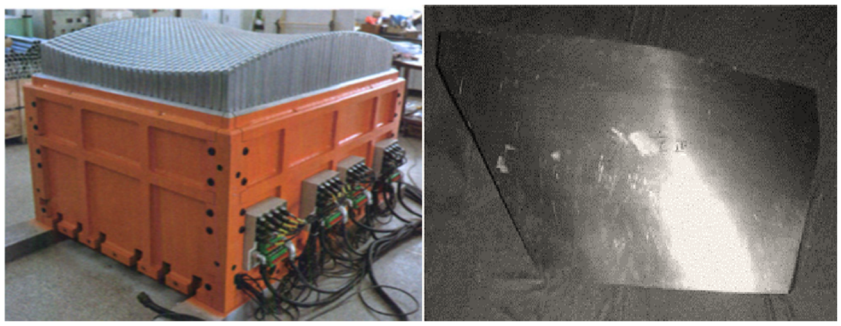

Fig. 8 Multi-point forming for sheet metal and the part formed by MPF [20]

and adding support structures [11–13]. Chen Yan et al. [14] presented a new method for automatically generating support structure for fabricating 3D objects with FDM printers. As shown in Fig. 5, compared with existing methods, such as Cura, MeshMixer and so on, the new algorithm can adjust the density and width of support structure to ensure stability and reliability in the printing process for models of different size, and it also reduces material cost and computation time. Nevertheless, it has difficulty in solving the construction interference of support structure.

The application of water-soluble material can save time in support structure removing because it can easily dissolve in special detergent making the post-processing simple, which smoothens the model surface [15–16]. When using water-soluble material, the printer needs two nozzles, one for build material and the other for support material, whose

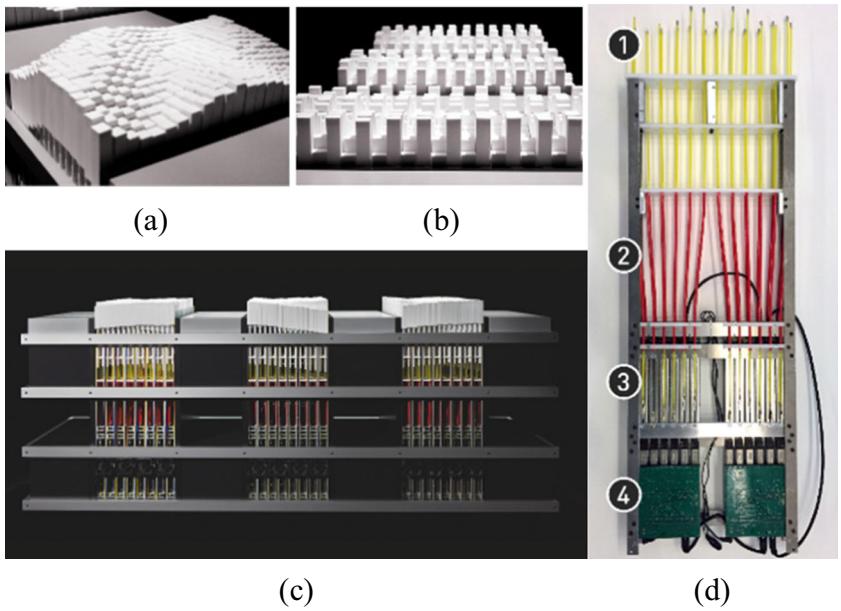

Fig. 9 Application modes and structure of TRANSFORM. **a** Wave mode. **b** Machine mode. **c** TRANSFORM side view. **d** Single engine module (2 ×12 pins). (1) Nylon rods that attach to the styrene pins, (2) plastic housing, (3) slide potentiometers, and (4) control boards] [21]

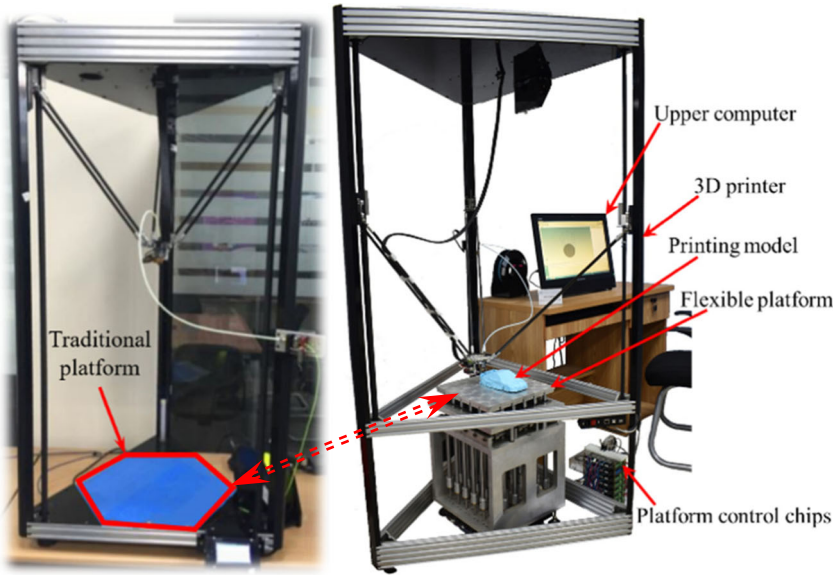

Fig. 10 The flexible platform in place of the traditional 3D printer's platform. **a** Traditional 3D printer. **b** Flexible platform work system

manufacturing accuracy is hard to guarantee [17]. But even worse, time and material during 3D printing are still wasted.

To solve the problem substantially, a concept of 5-axis FDM has been presented. Compared to the traditional 3D printer with three axes (X, Y, and Z), a 5-axis FDM printer has two extra axes (A and C) that allow work platform rotation, giving printing more freedom since the working plane can be adjusted to a suitable angle without adding support structure [18]. As shown in Fig. 6, William Yerazunis et al. [19] in the Mitsubishi Electric Research Laboratories (MERL) found out that there could be a typical strength improvement of 3× to 5× over conventional 3-axis parts printed to the same specification by laying down extrusions more closely aligned with the stress tensor within the part using a 5-axis 3D printer. However, a reliable 5-axis 3D printer requires complex mechanical structure and control strategies, so researchers should make more experiments to put it into practice.

For solving support structure, the support algorithm and support materials still waste time and material, and the 5-axis FDM printer's CAM is more complex than the traditional 3D printing CAM. This paper's idea is to look for external support to replace the original support structure. One or more supporting pieces are created in place of support structures, and then the model would be printed on them. In this way,

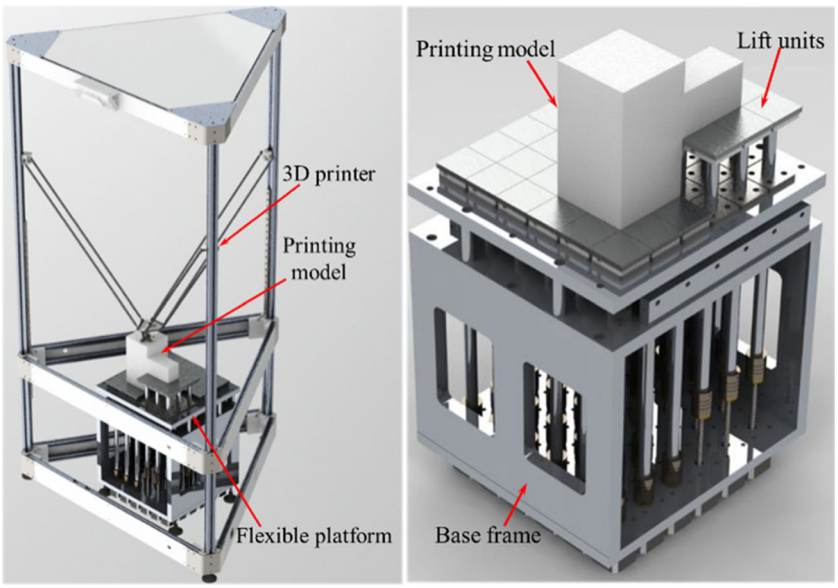

Fig. 11 3D models of the flexible platform work system. **a** Flexible platform work system. **b** Flexible platform

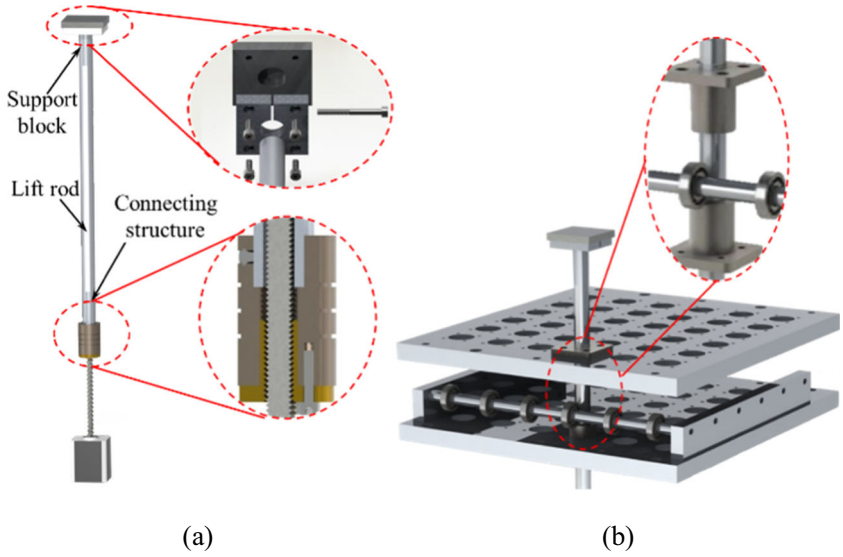

Fig. 12 Illustrations of important mechanical structure. **a** A lift unit. **b** The limit structure

time and material to print support structure can be saved. However, because different models have different support structures, and even different postures of the same model also have different support structures, it is hard to prepare enough supporting pieces in advance. As shown in Fig. 7b, if the supporting pieces are put before printing, it is very easy to bump the printer's nozzle on supporting pieces during printing, as the piece encroaches on the motion routes of the nozzle. Thus, it is necessary to come up with a flexible way of putting supporting pieces on the platform during the printing process.

The idea of forming of variable support structures is significant as a means of avoiding preparing different supporting pieces. Devices that fit the above concepts are used in other areas, such as multi-point forming (MPF) for sheet metal manufacturing and TRANSFORM, an intelligent furniture.

An MPF integrated system is described that can form a variety of part shapes without the need for solid dies,and given only geometry and material information about the desired part. As shown in Fig. 8, the central component of this system is a pair of matrices of punches with spherical ends, 28× 20 punches constructing an 840× 600 mm forming area and the

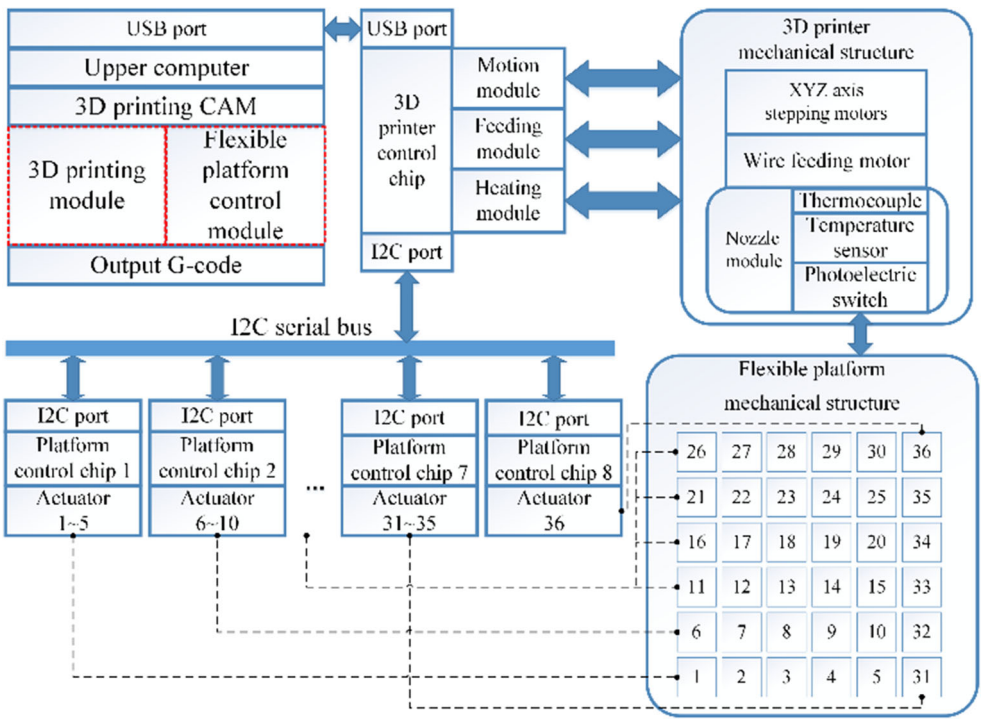

Fig. 13 An illustration of flexible platform control system structure

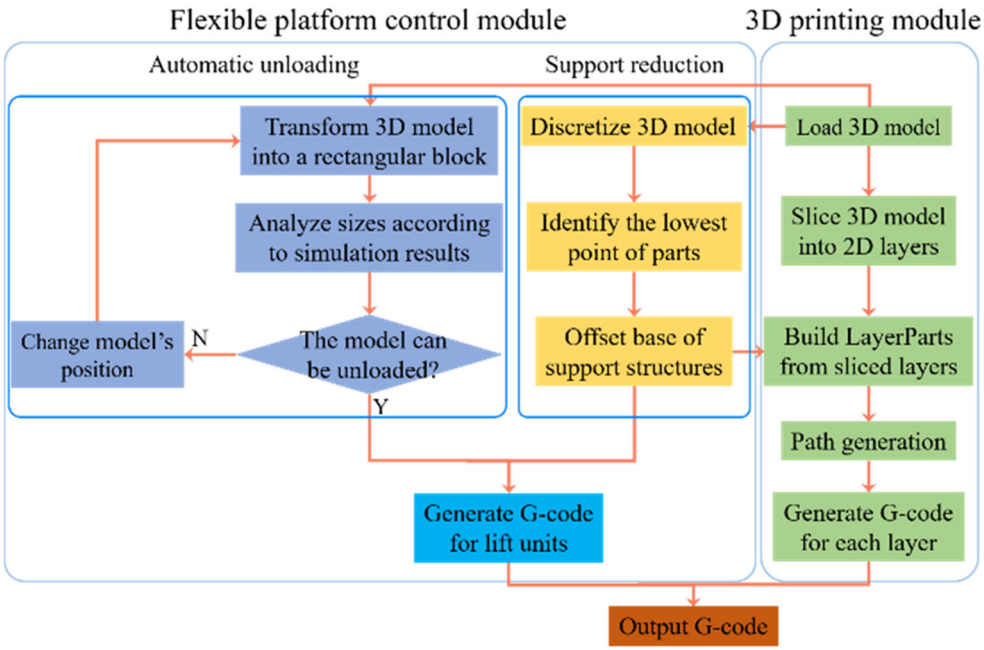

Fig. 14 G-code generation of the flexible platform control system

desired die surface is approximated by changing the positions of the punches through CAD and a control system [20].

Researchers at the MIT Media Lab invent the TRANSFORM, which enables transformation from a piece of static furniture to a dynamic machine driven by streams of data and energy, supporting a wide variety of activities. TRANSFORM is a platform based on actuator modules with 12× 2 styrene pins covering an area of 305×50.8 mm, which extends up to 100 mm from the surface. The modules can be seamlessly combined to form a larger shape display surface, 16×24 pins each, covering an area of 406.4×610 mm (Fig. 9c). The kinetic energy of the viewers, captured by sensors, drives the wave motion represented by the dynamic pins, which are controlled to move up and down in real-time to reshape the tabletop [21].

In this paper, a device, like the above, is introduced in 3D printing to form external support structure, which consists of small discretized pieces, called basic units, controlled to rise and fall by the upper computer. Hence, it can form different support structure using basic units to replace that generated by the 3D printer for different models. The collision can also be avoided by planning basic units' upward movement during the 3D printing process. What is more, in the last step of FDM process, basic units rise to pry the model from the platform to achieve the goal of automatic model unloading. As shown in Fig. 10, in comparison with the traditional 3D printer, the new 3D printer replaces the traditional platform with the device, named flexible platform.

The outline of this paper is organized as follows. In Section 2, the design of flexible platform work system is

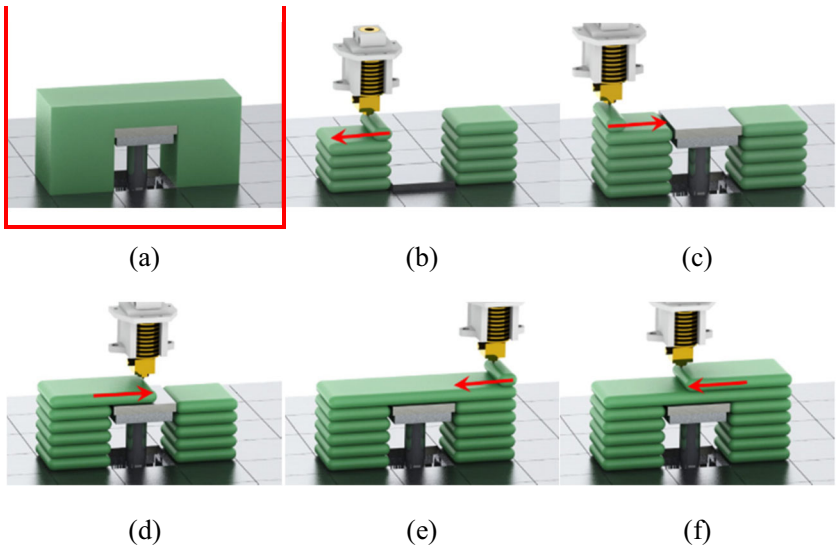

Fig. 15 Process for avoiding collision between the 3D printer and the flexible platform. The arrow shows motion direction of the 3D printer's nozzle

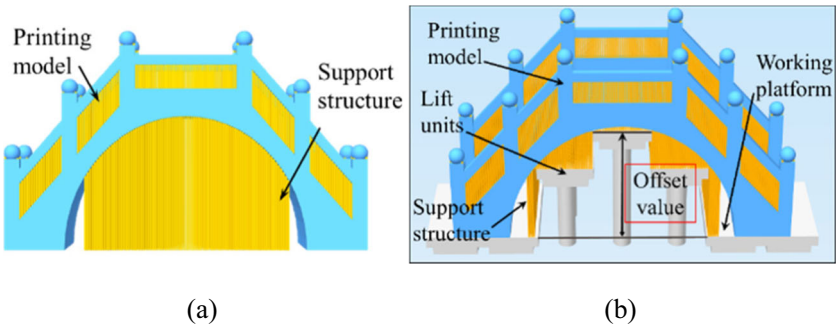

Fig. 16 Comparison between traditional support structure generating method and support structure reduction with flexible platform. (a) Support structure generated on the working platform; (b) Support structure generated on lift units of offset values in the height using flexible platform

introduced, including the structure, control module and process control. Section 3 presents implementation of support structure reduction, and two typical models are printed to verify the efficiency, and effect of the model's position on support structure reduction is studied. Section 4 gives a boundary of model's size between successful unloading and failure based on simulations and experiments, and the paper is concluded in Section 5.

2 Flexible platform work system

2.1 Structure and control design of the flexible platform system

As mentioned above, the traditional platform of a delta FDM printer is replaced by the flexible platform. The printing volume of the delta printer is a cylindrical space of 300 mm in radius and 800 mm in height. A photoelectric switch installed on the nozzle is used to measure initial heights of basic units of the flexible platform. As shown in Fig. 11b, the flexible platform consists of two parts, lift units and a base frame.

A lift unit with a 245-mm range takes up a square support area of the 50 mm side length, and the flexible platform's support area can be 300×300 mm. As shown in Fig. 12a, the lift unit is the basic unit of the flexible platform, distributed on a linear arrangement to reduce the occupied area, including a support block, a lift rod, a connecting structure and a stepping motor. The support block composed of two aluminum plates with bolts is mounted at the top of the lift rod, which is strictly perpendicular to the rod. The lift rod with a through-hole covers the linear stepping motor's screw. The connecting structure installed at the end of the rod connects the lift rod to the stepping motor. The stepping motor is the power source of the lift unit, and drives the unit up. The basic frame plays important roles in load bearing and guiding, where installation holes are designed for lift units. As shown in Fig. 12b, the limit structure is located at the top of the frame, which ensures accuracy of motion. Flanges on the two limit boards guarantee the stiffness of the mechanism in the vertical direction. Outer ring of the rolling bearing props the surface in the side of the lift rod, limiting the rotation of the lift rod around the Z axis.

As shown in Fig. 13, flexible platform control system consists of an upper computer, a 3D printer and a flexible platform. The 3D printing CAM in the upper computer integrated with the 3D printing module and the flexible platform control module generates G-codes to achieve motion control. The 3D printer not only receives instructions, but also sends location,

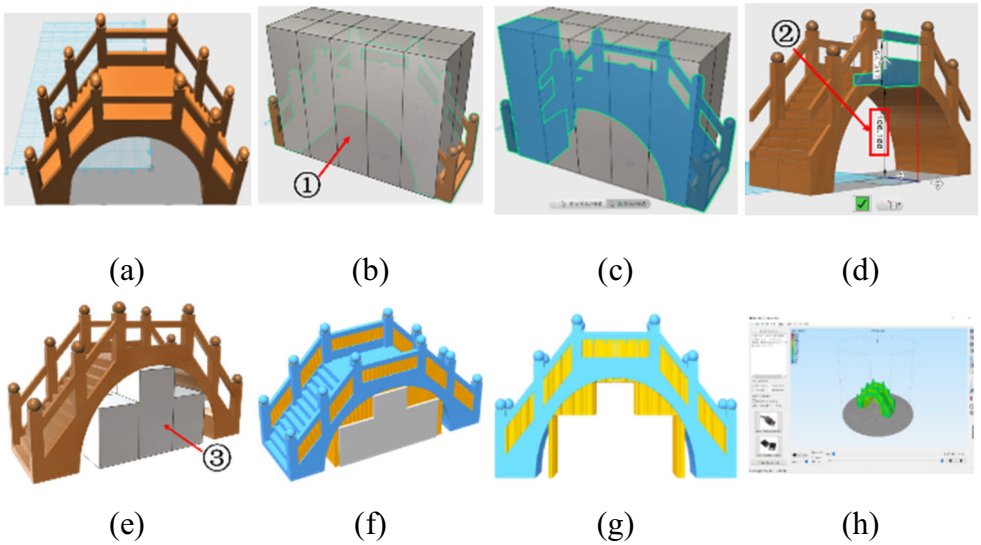

Fig. 17 The implementation process of support structure reduction. **a** Importing model. **b** Lift unit array generation. **c** Discretizing the model. **d** Getting the offset value of each part. **e** Forming the external support with deformed cubes. **f** Generating support structure on the cubes. **g** Getting the model after support reduction. **h** Generating instructions. [(1) Lift unit array. (2) Offset value. (3) Deformed cubes]

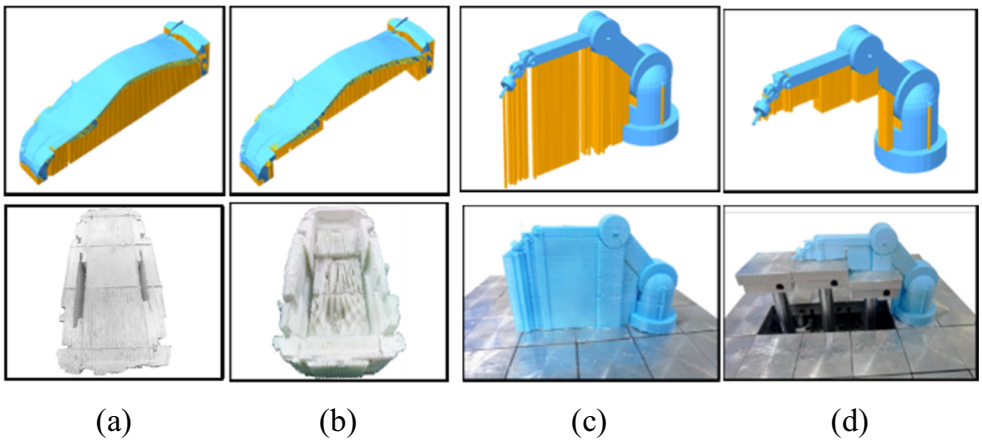

Fig. 18 Comparison between the models of reduced support structure and full support structure. The upper row shows the simulation results and the lower row shows the printed models

temperature and other messages measured by sensors to the upper computer using the USB port. After being encrypted in the 3D printer control chip, the instructions are transferred to the platform control chips through the I2C serial bus. A photoelectric switch in the 3D printer measures initial heights of lift units of the flexible platform and then feedbacks the information to the upper computer for reference of adjustment.

As shown in Fig. 14, the 3D printing module and the flexible platform control module generate G-code together. The flexible platform control module includes support structure reduction and automatic unloading. Support structure reduction mainly includes 3 steps. The first step is to discretize the model's printing space to pieces. The second step is to identify the lowest point of each piece. The third step is to offset the base of support structure. The support structure reduction instruction is output and at the same time, the information about decrement of support structure is transferred to 3D printing module. Automatic unloading also includes 3 steps. The first step is to approximately transform the model into a rectangular block. Secondly, the model's sizes are analyzed according to simulation results. If the condition is met, the unloading instruction is output. Otherwise, the original position of the model is changed until the instruction can be output. Further details will be discussed in the following sections.

2.2 Process control

As mentioned above, the collaboration between the 3D printer and the platform needs to avoid collision at first. Therefore, process control should be introduced to avoid it. For example, Fig. 15a shows a model with cantilever structure supported by a lift unit. As shown in Fig. 15b, the 3D printer is printing one layer before the cantilever structure, when the lift unit to support the structure is ready to rise. Then, Fig. 15c shows that when the unit arrives at the destination, the printer is printing the cantilever structure. Specifically, according to 3D printing's process which fabricates parts through adding material layer by layer, the process control can be achieved if the platform control G-code is inserted before the corresponding code of printing the cantilever structure. At the same time, the insertion of code should be concerned with the factors such as the unit lifting speed and the printer printing speed.

3 Support structure reduction

The FDM printer must generate support structure to support the cantilever structure, which wastes time and material. The flexible platform forms external support in place of support structure by numerically controlling lift units to rise to a certain height, which meets demands of different models.

3.1 Implementation of support structure reduction

Generating G-codes to control the motion of the printer and the flexible platform is the key of implementation of support structure reduction. In contrast to the traditional way, new methods for generating G-codes should consider about the path generation of the 3D printer after support structure reduction and lift unit movement during printing process. As shown

Table 1 Typical models' printing results of reduced support structure and full support structure

Test parameters	Car shell			Robotic arm		
	Full	Reduced	Reduction rate	Full	Reduced	Reduction rate
Printing time	15 h 23 min	10 h 32 min	31.53%	6 h 23 min	4 h 2 min	36.81%
Model's weight	195.60 g	137.10 g	29.91%	74.10 g	43.65 g	41.09%

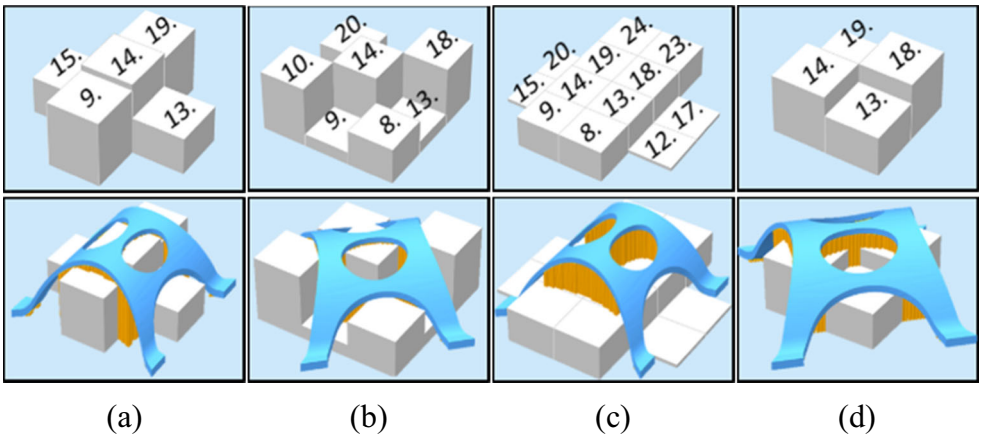

Fig. 19 Studying effects of model's position on support structure reduction. The upper row shows deformed cubes and the lower row shows the models with reduced support structure

in Fig. 16a, the conventional model for 3D printing has support structure generated on the platform of 0 mm in the height. If the flexible platform is used to assist manufacture, the support structure of the model will be cut off the volume of lift units. As shown in Fig. 16b, the lift unit, where support structure is generated, has its maximum height decided by the relative position between the model and the platform. The height called the offset value of support structure is significant to the new way for path generation of 3D printing, and it also guides the instructions that are used to control the motion of the lift units.

As shown in Fig. 17, the implementation process of support structure reduction includes eight steps. At first, the model is introduced to the working coordinate system in a fixed location. Secondly, arrays of lift units in the corresponding location are imported into the software. The third step is the intersection of the units' arrays with the model, which discretizes the model into small parts. In the fourth step, the maximum height of each lift unit is acquired, which is the Z coordinate value of the bottom of the partial model. Fifthly, the cube, the same size as the lift unit, rises to the height acquired in the fourth step, which is combined with the model. The sixth step is generating support structure on the cubes. In the seventh step, the cubes are removed to get the model after support structure reduction. In the end, the model is sliced to generate the codes to control motion of the FDM printer. The last four steps are equivalent to subtracting the supporting structure's three-dimensional file. In addition, in practical applications, it is necessary to leave residual amount between the lift units to avoid interference on the boundary of lift units during the printing process.

3.2 Two typical models for printing with the flexible platform

Support optimization of flexible platform is mainly on reducing material and improving efficiency of printing, so in this paper two typical models for printing with the flexible platform were printed to verify the function and performance. The cantilevered model and the shell-structure model both require a lot of support structure. As shown in Fig. 18, a car shell model and a robotic arm model were printed as test pieces.

The test parameters included printing time and the weight of the models, which reflected the printing efficiency and the material consumption. Then, the comparison between the model of reduced support structure and full support structure was adopted. Table 1 shows printing results of two tests. The reduction rate of the test reaches about 30%, which preliminarily identifies the effectiveness and feasibility of printing using the flexible platform.

3.3 The effect of the model's position on support structure reduction

The position of the model determines the offset value of support structure in each region, thus affecting the support structure reduction. The paper chose the arch-type model as the research object to study the influence rule. As shown in Fig. 19, the model was changed position by translation and rotation transform, which obtained four kinds of support structure. The cubes in the upper row rose to the height of the offset value in the corresponding region, which was attained after the steps 1–4 of the process mentioned above; and the number on cubes indicated lift units' serial number. In the lower figures, the model with its reduced support structure generated on the cubes. The test parameters of the prediction generated by 3D software, which resulted close to the actual values, are listed in Table 2.

Table 2 Predictions of printing results about model's position on support structure reduction. Italicized entries show the optimal scheme

Test parameters	#1	#2	#3	#4
Printing time	*7 h 4 min*	8 h 53 min	7 h 15 min	7 h 25 min
Model's weight	*90.01 g*	116.33 g	96.29 g	93.47 g

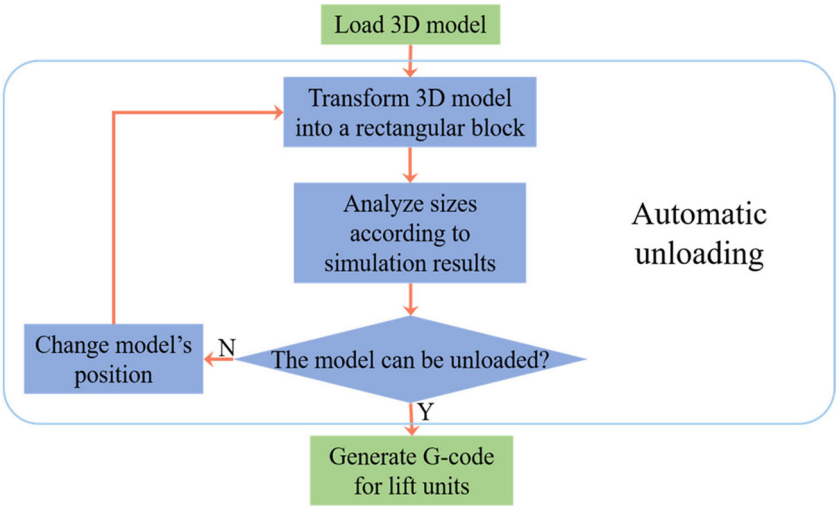

Fig. 20 Steps of automatic unloading using the flexible platform

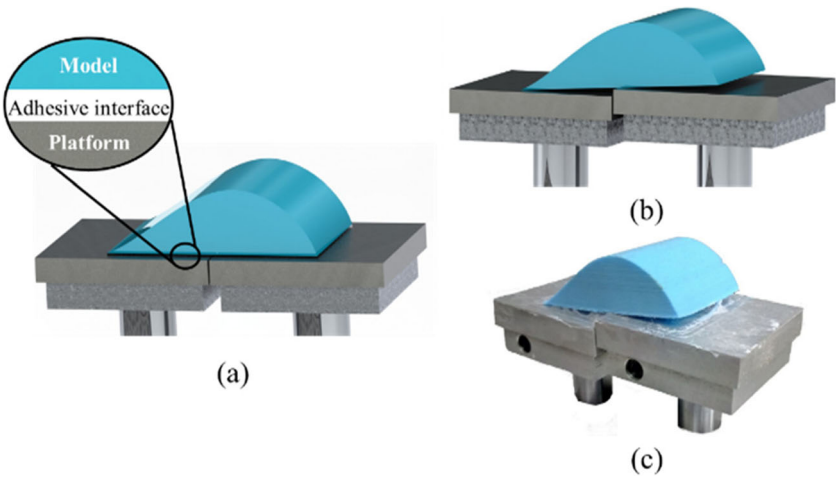

Fig. 21 Small-bottom model unloading process

By comparison of four kinds of support structure reduction, the first one was the optimal scheme, whose values were smallest among the test parameters. There was an interesting point in the comparison between the parameters of the third and the fourth. Though printing time of the third cost less, weight of the fourth was of lower value. Therefore, the two parameters were not strictly correlated, and were affected by factors such as position and the model's shape, which meant

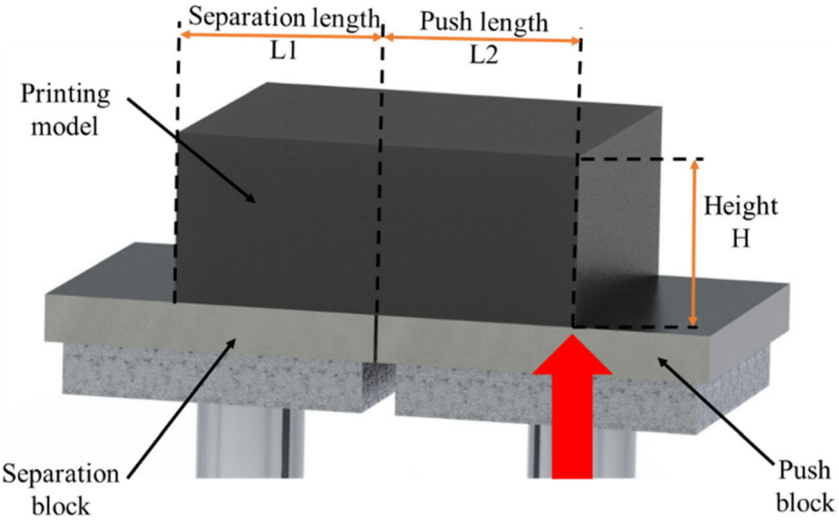

Fig. 22 A basic rectangular block transformed by a small-bottom model with key parameters

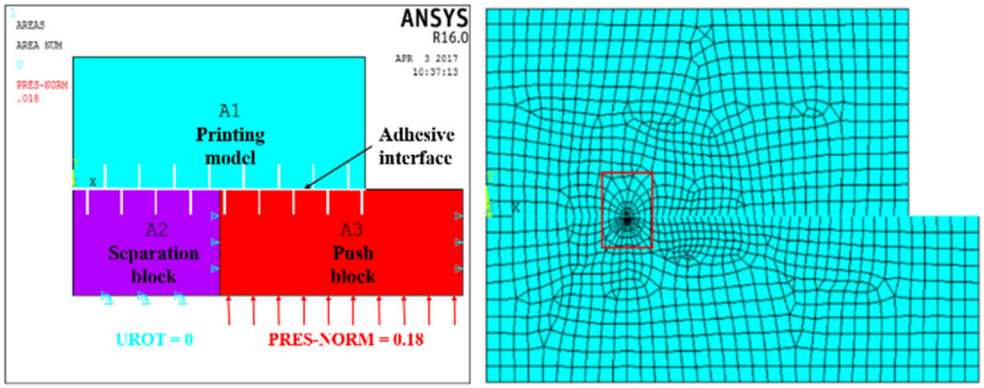

Fig. 23 The constraint condition and grid division of the simulation model

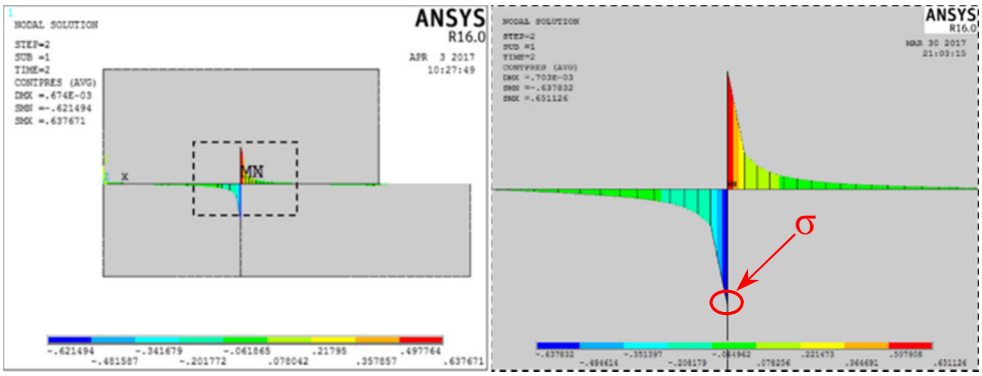

Fig. 24 The distribution of pressure on the adhesive interface of the simulation model

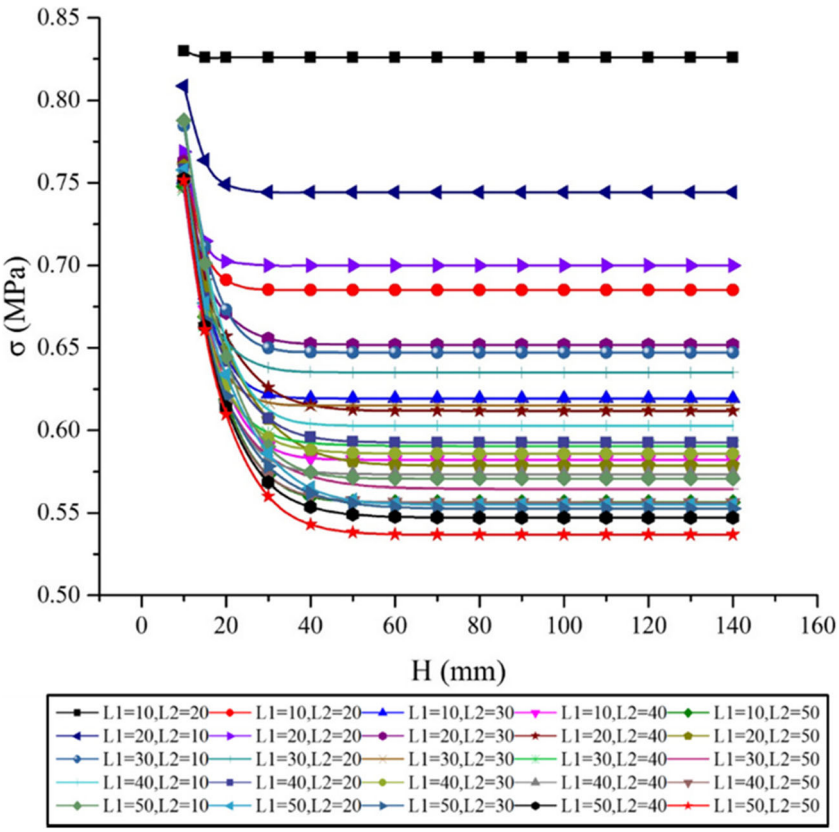

Fig. 25 Curves of effects of parameter combinations on maximum pressure, σ_p

Table 3 Orthogonal experimental design to find the theoretical unloading threshold. As shown in italics, the theoretical unloading threshold is found between #15 and #19

$L_{25}(5^3)$ Experiment	Influencing factor			σ_p (MPa)	Separate (Yes/No)
	L1(mm)	L2(mm)	H(mm)		
#1	10	10	10	0.82992	Yes
#2	10	20	15	0.70941	Yes
#3	10	30	20	0.64458	No
#4	10	40	30	0.59062	No
#5	10	50	40	0.55986	No
#6	20	10	15	0.76374	Yes
#7	20	20	20	0.70243	Yes
#8	20	30	30	0.65555	No
#9	20	40	40	0.61541	No
#10	20	50	10	0.76032	Yes
#11	30	10	20	0.67318	Yes
#12	30	20	30	0.63817	No
#13	30	30	40	0.61518	No
#14	30	40	10	0.74620	Yes
#15	*30*	*50*	*15*	*0.66131*	*No*
#16	40	10	30	0.61255	No
#17	40	20	40	0.59610	No
#18	40	30	10	0.75419	Yes
#19	*40*	*40*	*15*	*0.66530*	*Yes*
#20	40	50	20	0.61488	No
#21	50	10	40	0.57467	No
#22	50	20	10	0.75775	Yes
#23	50	30	15	0.66691	Yes
#24	50	40	20	0.61409	No
#25	50	50	30	0.56007	No

that the impact of both parameters should be considered when giving the best scheme for support structure reduction.

4 The automatic unloading process

As shown in Fig. 20, the automatic unloading process includes the following steps. In the first step, the model is imported into the software and placed in the initial position. The second step is to approximately transform the model into a rectangular block. Thirdly, the model's sizes are analyzed according to simulation results. If the condition is met, the unloading instruction is output. Otherwise, the original position of the model is changed until the instruction can be output. The following of the section introduces the simulation and related experiments. At last, parameters of successful unloading are given based on the simulation and experiments.

4.1 Unloading process simulation for model with small bottom

Small-bottom model unloading is the base of model unloading, from which the large-bottom model unloading can be deduced. As shown in Fig. 21, a small-bottom model's bottom area is less than two lift units' size and the model can be separated from the flexible platform with one unit rising. There is an interface between the model and the platform, which is the barrier to model unloading. Glue is used to enhance the interface strength to prevent the warp during the printing process. Therefore, the whole unloading process can be thought as the use of the lift unit uplifting to destroy the adhesive interface as shown in Fig. 21c.

The critical stress state of the interface was simulated by ANSYS on the assumption that the model was not separated from the platform. In the simulation, the small-bottom model was approximately simplified into a rectangular block; and the lift unit to push the model up was recorded as the push block, while the stationary unit was the separation block. As shown

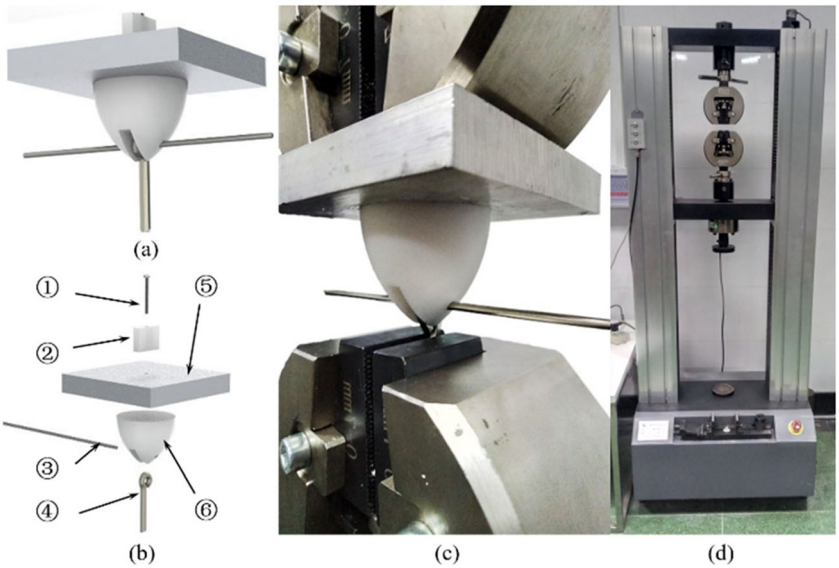

Fig. 26 Tensile tests with test pieces to measure the actual pressure value. **a** Test piece. **b** Composition of the test piece. [(1) Bolt. (2) Clamp block. (3) Latch. (4) Cheek. (5) Aluminum block. (6) Dome-shaped print model with the base diameter of 50 mm]. **c** The tensile test of test pieces. **d** The universal testing machine

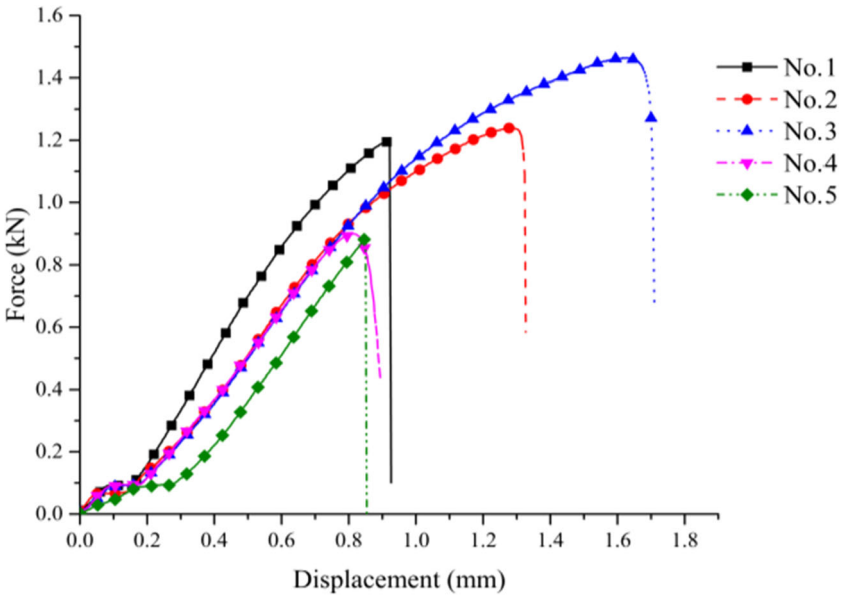

Fig. 27 Force-displacement curves of the tensile tests

in Fig. 22, the key parameters of the simulation model include the separation length L1, the push length L2, and the model thickness H. The width of the model was set 50 mm, equal to the width of the unit, so that the simulation simplified the analysis to two-dimension.

As shown in Fig. 23, the simulation model includes three parts: the printing model A1, the separation block A2 and the push block A3. The behavior of contact surface between the printing model and the flexible platform was set Bonded(Always),which was used to represent the adhesive interface. For simulating the actual motion, the degree of freedom at the bottom of the separation block and on the sides of the push block was set 0. The push block, whose bottom surface was under uniform pressure with a value of 0.18 MPa, was driven by the step motor. During the meshing, the boundary among the printing model, the separation block and the push block needed to be refined because this was where the fracture occurred.

Figure 24 shows the distribution of pressure on the adhesive interface of the simulation model. The absolute value of the pressure had a maximum at the boundary and the value decreased with an exponential function as the distance increased. The model was stretched on the separation block, so the maximum pressure, called σ_p, was negative, which had an important impact on unloading.

4.2 Unloading threshold

More practical conclusions needed to be found guiding the unloading, and in other words, the unloading threshold should be expressed in a numerical way.

To begin with, the paper would analyze how those key parameters effected σ_p.As shown in Fig. 25, the model thickness H is set as the main parameter, and the separation length L1 and the push length L2 are secondary parameters. The pressure values, σ, were obtained by the simulation analysis of different parameter combinations (H, L1 and L2). With a set of L1 and L2 values and the changing value of H, the pressure value would decrease to the limit value as H increased. Different sets of L1 and L2 values changed the limit value.

Secondly, the theoretical pressure threshold of the actual fracture was studied. Orthogonal experimental design L_{25} (5^3), listed in Table 3, was introduced to reduce the number of experiments. In Fig. 25, when H exceeded 40 mm, the pressure value was close to the limit value, and thus, the parameter H was selected from 10 to 40 mm. The pressure value σ_p, listed in the left side of Table 3, was from simulation results in Fig. 25. The experiment was taken to check whether the test model would be separated with the experiment combinations listed in Table 3.

The experiment was introduced as follows: according to selected parameter combinations, the test model, like a rectangular block shown as in Fig. 22, was printed. The lift units' surface was coated with glue according to practice in Fig. 21 and stood for 4 h after solidification. Then, the push block was commanded to move up. At last, the separation result of the model was recorded. As shown in Table 3, separation results have close correlation with the pressure value σ_p. The theoretical unloading threshold, about approximately 0.6633 MPa, is

Table 4 Maximum loads of tests recorded by the universal testing machine

	No.1	No.2	No.3	No.4	No.5
Force/kN	1.197	1.241	1.464	0.900	0.887

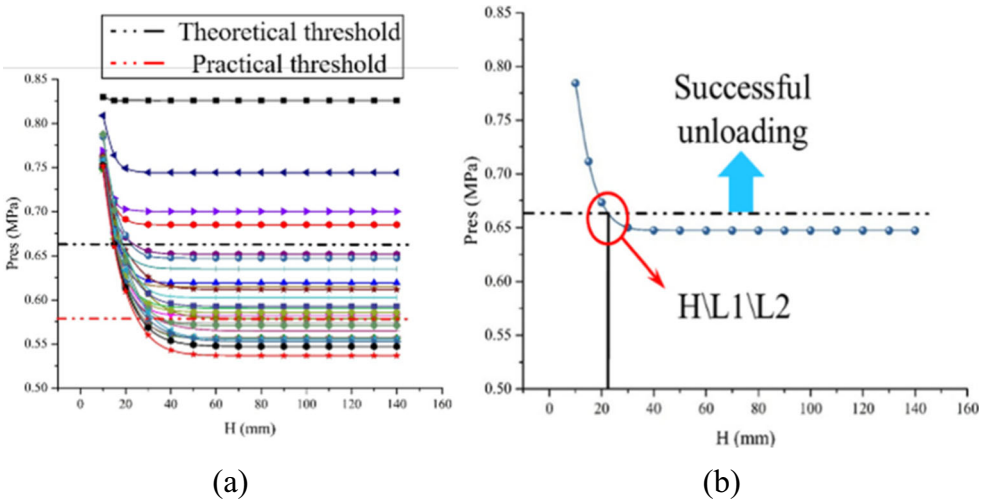

Fig. 28 Defining the relationship between the model parameters and threshold values

found between #15 and #19. It divides the parameter combinations into the successful separation and the failure.

At last, the following was an experiment on measuring the actual pressure value. As shown in Fig. 26, special test pieces were designed to carry out tensile tests, whose main body consisted of a dome-shaped printing model, an aluminum block and some connectors. Like the manufacturing process of the model in Fig. 21, the test model was printed on an aluminum block: The first step was to fix the aluminum block in the center of the 3D printer's working platform. The second step was to apply glue evenly over the surface of the aluminum block. The third step was to print the test model on the aluminum block's surface coated with glue. The last step was to install connectors on the test model and the aluminum block to form the test piece. The printing process of test models was carried out under the room temperature, and the test pieces were kept for 4 h before the tensile test. The tensile test was carried out with a universal testing machine in the laboratory, whose top chunk clamped the clamp block of the test piece and the bottom chunk clamped the cleek of the test piece. On the base of ensuring that the force line was perpendicular to the glue interface, the clamping device stretched the sample at the speed of 2 mm/min. The measurement was not terminated until the interface was damaged at the maximum load.

As shown in Fig. 27, five test pieces were measured on a universal testing machine and the curves recorded by the

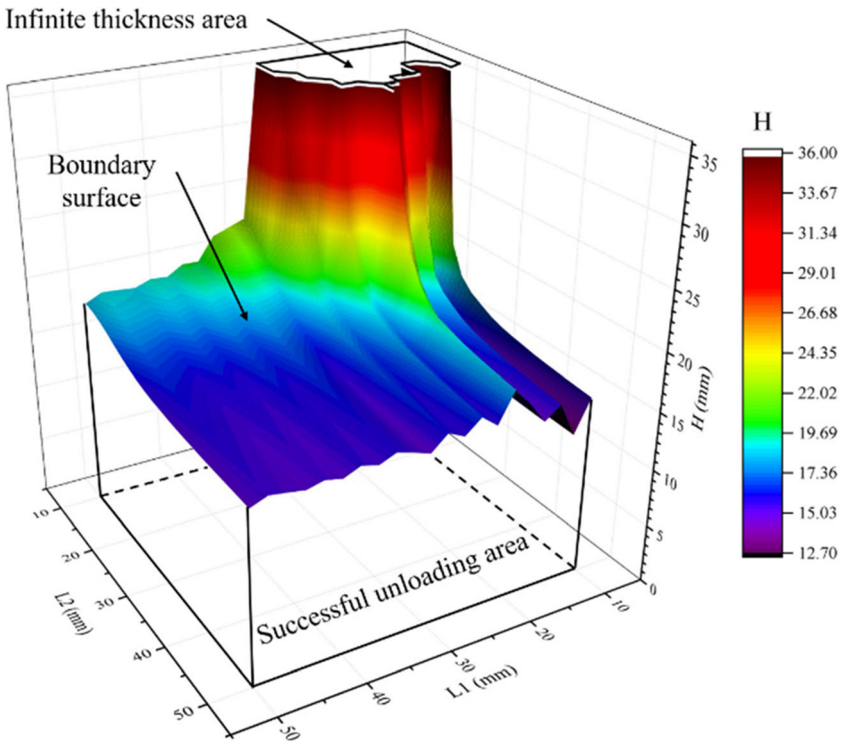

Fig. 29 Successful unloading parameter area in the parameter space

machine are presented below. Maximum loads are listed in the Table 4. Each curve displays the same properties and adhesion failure was the main failure type of each test piece. Though the maximum loads vary from tests, the fluctuation of the results is acceptable due to the existence of the 3D printing's error. After the experiment value was processed, the adhesive force value was obtained, and then the actual pressure value was obtained via dividing force by the bottom area of the test model, which was about 0.5875 MPa.

4.3 The successful unloading parameter area

Though the theoretical and practical thresholds were attained, it was hard to directly use those to guide the unloading. Because the size of the model was received more often in the 3D printing software, the relationship between the model size and threshold values needed to be defined.

As shown in Fig. 28, the unloading threshold line went across curves, which divided the curve into two parts. The part above the line could be successful unloading because it meant greater pressure value than the threshold. Conversely, the part below the line could mean failure because of lower pressure value. In addition, the line had an intersection with the curve, which was a part of boundary between successful unloading and failure.

Thus, the combination of parameters related to the intersections was mapped into the parameter space, whose coordinates were L1, L2 and H. As shown in Fig. 29, the colorful boundary surface and its below were areas of successful unloading. There was a strange place, infinite thickness area, where the value of model thickness could be infinite as the thickness was not the major factor anymore.

5 Conclusion

Support structure and model unloading are two major obstacles for development of FDM. This paper designed a kind of flexible platform to assist FDM printing. Four main achievements have been made in this work.

(1) The mechanical design scheme of 3D printing support flexible platform has been put forward, which consists of lift units and a base frame. The lift unit was controlled by the linear stepping motor to rise and fall, and the basic frame played important roles in load bearing and guiding.

(2) To meet the requirement of the flexible platform's printing system, the control system of the flexible platform has been developed. The collision between the printer nozzle and lift units was avoided by controlling lift units' movement.

(3) After implementation of support structure reduction, typical models have been printed to verify efficiency of the method, and experiments have been designed to study the influence of model's position on support structure reduction.

(4) Combining theoretical analysis and experimental verification, the law of model unloading has been studied. The unloading process was simulated to study the stress state and then the mechanical test was put into effect to measure the actual value. In the end, the parameters of successful unloading were given to guide the unloading process.

Funding information This work was financially supported by the National Natural Science Foundation of China (No. 51475421), the Science Fund for Creative Research Groups of National Natural Science Foundation of China (No. 51521064), and Key research and development plan of Zhejiang Province (No.2018C01073).

References

1. Economist (2012) "A third industrial revolution", Economist Magazine Special Report, 21 April 2012
2. Carneiro OS, Silva AF, Gomes R (2015) Fused deposition modeling with polypropylene. Materials & Design 83(4):768–776
3. Bernard A, Fischer A (2002) New trends in rapid product development. CIRP Ann Manuf Technol 51(2):635–652
4. Faludi J, Bayley C, Bhogal S, Iribarne M (2015) Comparing environmental impacts of additive manufacturing vs traditional machining via life-cycle assessment. Rapid Prototyp J 21(1):14–33
5. Perry N, Mognol P, Lepicart D (2014) Rapid prototyping: energy and environment in the spotlight. Rapid Prototyp J 12(1):26–34
6. Lee J, Lee K (2016) Block-based inner support structure generation algorithm for 3d printing using fused deposition modeling. Int J Adv Manuf Technol 89(5–8):1–13
7. Ali MH, Mir-Nasiri N, Ko WL (2016) Multi-nozzle extrusion system for 3d printer and its control mechanism. Int J Adv Manuf Technol 86(1–4):999–1010
8. Mohamed OA, Masood SH, Bhowmik JL (2015) Optimization of fused deposition modeling process parameters: a review of current research and future prospects. Advances Manufacturing 3(1):42–53
9. Kulkarni P, Marsan A, Dutta D (2000) A review of process planning techniques in layered manufacturing. Rapid Prototyp J 6(1): 18–35
10. Volpato N, Aguiomar Foggiatto J, Coradini Schwarz D (2014) The influence of support base on FDM accuracy in Z. Rapid Prototyp J 20(3):182–191
11. Allen, S., & Dutta, D. (1995). Determination and evaluation of support structures in layered manufacturing. Journal Ofdesign & Manufacturing, 5
12. Snead, D. E., Smalley, D. R., Cohen, A. L., Allison, J. W., Vorgitch, T. J., & Chen, T. P. (2001). Boolean layer comparison slice US, US6333741
13. Huang X, Ye C, Wu S, Guo K, Mo J (2009) Sloping wall structure support generation for fused deposition modeling. Int J Adv Manuf Technol 42(11–12):1074–1081
14. Chen Y, Wang SW, Yang ZW, Liu LG (2015) Construction of support structure for FDM 3d printers. Scientia Sinica Informationis 45(2):259
15. Masood SH, Song WQ (2004) Development of new metal/polymer materials for rapid tooling using fused deposition modelling. Mater Des 25(7):587–594

16. Iv RWG, Baird DG, Bøhn JH (1998) Effects of processing conditions on short TLCP fiber reinforced FDM parts. Rapid Prototyp J 4(1):14–25
17. Xu K, Zhang J, Wuhan (2008) A study of the support technology in fused deposition modeling. Mechanical Sci Technol Aerospace Engineering 27(9):1163–1166
18. Grutle ØK (2015) 5-axis 3D printer. University of Oslo, Dissertation
19. Yerazunis, W.S., BarnwellIII, J.C.,Nikovski, D.N.. Strengthening ABS, Nylon, and Polyester 3D Printed Parts by Stress Tensor Aligned Deposition Paths and Five-Axis Printing. MITSUBISHI ELECTRIC RESEARCH LABORATORIES. http://www.merl.com. August 2016
20. Li MZ, Cai ZY, Sui Z, Yan QG (2002) Multi-point forming technology for sheet metal. J Mater Process Technol 129(S1):333–338
21. Ishii, H., Leithinger, D., Follmer, S., Zoran, A., Schoessler, P., & Counts, J. (2015). TRANSFORM: Embodiment of "Radical Atoms" at Milano Design Week. In Proceedings of the 33rd Annual ACM Conference Extended Abstracts on Human Factors in Computing Systems (CHI EA '15). ACM, New York, p 687–694